



Soft Matter

**Supramolecular fibrous gels with helical pitch tunable by
polarity of alcohol solvents**

Journal:	<i>Soft Matter</i>
Manuscript ID	SM-ART-12-2020-002136
Article Type:	Paper
Date Submitted by the Author:	02-Dec-2020
Complete List of Authors:	Iwaura, Rika; National Agriculture and Food Research Organization, National Food Research Institute Komba, Shiro; National Agriculture and Food Research Organization, Food Research Institute Kajiki, Takahito; Sunus Co. Ltd., Research and Development

SCHOLARONE™
Manuscripts

Supramolecular fibrous gels with helical pitch tunable by polarity of alcohol solvents

Rika Iwaura ^{*a}, Shiro Komba ^a, and Takahito Kajiki ^b

^a Drs. R. Iwaura and S. Komba

Food Research Institute, National Agriculture and Food Research Organization

2-1-12 Kannondai, Tsukuba, Ibaraki 305-8642, Japan

^b T. Kajiki

SUNUS Co., Ltd.

3-20 Nan-ei, Kagoshima, Kagoshima 891-0196, Japan

* E-mail: riwaura@affrc.go.jp

Abstract

A sugar-based, low-molecular-weight gelator 16AG, can gelatinize primary alcohols by forming supramolecular fibers. We obtained non-helical, tape-like fibers in methanol and ethanol but helical fibers in alcohols with at least three carbons. The pitch of the helical fibers became shorter with increasing carbon number.

1 Introduction

Supramolecular chirality is common in biological molecules, including the DNA double helix and folded proteins; chiral structures are often involved in important biological functions, for example, storage of genetic information or antigen–antibody binding. Constructing and controlling the desired chiral morphology by the self-assembly of molecular building blocks remains a great challenge for chemists despite much effort having been devoted to the development of supramolecular systems for this purpose.¹⁻⁹ In such systems, building-block molecules assemble by non-covalent interactions such as hydrogen bonding and hydrophobic, electrostatic, and π - π stacking interactions, and form nano-to-meso-scale chiral supramolecular structures. The chirality of supramolecular assemblies can be controlled by enantioselective syntheses of the building-block molecules¹⁰⁻¹² or by chiral amplification by chiral dopants.¹³⁻¹⁵ Thus, the design of the building-block molecules is crucial for the control of supramolecular chirality.

Solvent is another important factor for supramolecular chiral structure construction.^{16, 17} During self-assembly, the properties of the solvent molecules, for example their polarity, affect the building-block molecules. In nonpolar solvents, the polar moieties of these molecules avoid contact with the solvent; similarly, their non-polar moieties in a polar solvent avoid contact with solvent molecules. In different solvents, the same building-block molecules may form different supramolecular structures or give rise to different supramolecular chirality. Solvent-dependent chiral morphology construction¹⁸⁻²⁶ and solvent-tuned supramolecular chirality²⁷⁻³² have been reported, demonstrating the feasibility of construction and tuning of various chiral structures from

the same building-block molecule by taking advantage of the effect of solvent. In particular, the report of Liu et al.²², in which the pitch length of a nanotwist and a helical structure were tuned depending on the content of water, demonstrated well that a subtle change in solvent can trigger a change in supramolecular chirality. However, the interactions between the building-block molecules and solvent are diverse and complex, and the role of the solvent is still not clearly understood.

We have reported that 1,5-anhydro-2,3,4,6-tetra-*O*-palmitoyl-D-glucitol (16AG), a palmitoylated derivative of 1,5-anhydro-D-glucitol (Table 1), which was synthesized enzymatically from starch, gelatinized various organic solvents by the formation of self-assembled fibers via the solvophobic effect and CH \cdots O hydrogen bonding.^{33, 34} In this study, we carried out supramolecular gelation of 16AG using a homologous series of primary alcohols whose polarities are decreasing with increasing number of carbons, as solvents. We report here the systematic changes of the helical pitch and sol-to-gel phase transition temperature (T_{gel}) of supramolecular fibrous gels formed from 16AG depending on solvent polarity and reveal that the solvent is important in the formation of chiral structure and phase transition temperature of the supramolecular assembly. Based on these findings, we also demonstrate that the helical pitch and T_{gel} of supramolecular fibrous gels can be tuned in a mixture of solvents with different polarities.

Table 1

2 Experimental section

2.1 Materials. The synthesis and compound analyses of 1,5-anhydro-2,3,4,6-tetra-*O*-palmitoyl-D-glucitol (16AG) were reported previously.³⁴ Primary alcohols were purchased from Tokyo Chemical Industry Co., Ltd. (Tokyo, Japan) and used without further purification.

2.2 Preparation of fibrous gels in primary alcohols. 1,5-Anhydro-2,3,4,6-tetra-*O*-palmitoyl-D-glucitol (5 mg) was added to 500 μ l of primary alcohol, and the mixture was heated at 80°C for 10 min and then allowed to cool to room temperature.

2.3 Optical microscopy. Gel sample was placed on a glass slide and covered with a cover slip. Optical images were recorded under a differential interference contrast mode (BX51) equipped with a 3-CCD video camera (CS520MD; both from Olympus, Tokyo, Japan).

2.4 Variable-temperature transmittance spectroscopy. The transmittances of the samples containing 16AG in alcohol solvents were monitored with a UV-1800 spectrophotometer equipped with a TMSPC-8 thermal melt analysis system (Shimadzu Corp., Kyoto, Japan) at a cooling rate of 0.5°C min⁻¹.

2.5 X-ray diffraction analysis. Fibrous gel samples in alcohol were placed in glass capillary tubes, and their X-ray diffraction patterns were obtained with a Rigaku diffractometer (Type 4037; Rigaku, Tokyo, Japan) by using graded *d*-space elliptical side-by-side multilayer optics, monochromated CuK α radiation (40 kV, 30 mA), and an

imaging plate (R-Axis IV; Rigaku, Tokyo, Japan). The exposure time was 30 min, and the camera length was 150 mm.

2.6 Variable-temperature circular dichroism spectroscopy. Circular dichroism spectra were recorded on a J-820 (Jasco Corp., Tokyo, Japan) instrument in a 0.1-mm quartz cell. The samples were equilibrated at each temperature for 5 min before measurements.

3 Results and discussion

3.1 Optical and atomic force microscopy observations of organogels formed from 16AG in primary alcohols. Samples of 16AG (1 mg) were dissolved in 100 μ l of each alcohol by heating at 80°C and kept at room temperature. After several minutes to several tens of minutes, we obtained opaque gels from all the samples, and the delay of the gelation increased consistently with the increasing number of carbons in the alcohol. The gel that formed in methanol but not in the other alcohols expelled small amounts of solvent after several hours. Optical microscopy revealed formation of fibers whose morphologies depended on the alcohol used (Figure 1, Figure S1 a-j). Fibers formed in methanol and ethanol displayed tape-like morphology (width, ca. 1 μ m) and were slightly twisted (Figure 1 a, b). All fibers that formed in alcohols with ≥ 3 carbons had helical structures. This observation was supported by the fact that the CD spectra of gels produced in methanol and ethanol were silent, but a positive band in the absorption wavelength region of 16AG (<250 nm) was present in alcohols having 3 or more carbon atoms (Figure S2). However, the pitch of the fibers depended on the alcohol used (Table

1, Figure S3 a): a mean pitch of the fibers was ca. 3.3 μm in 1-propanol and decreased with increasing carbon number (e.g., 1-hexanol, ca. 1.3 μm ; 1-nonanol, 1.0 μm). To further analyze the structure of the fibers, we used atomic force microscopy. Fibers formed in methanol had tape-like morphology with a width of ca. 1 ~ 2 μm (Figure 2a), similar to that revealed by optical microscopy; each tape-like fiber was hierarchically constructed from fibers with a minimum height of ca. 60 nm (Figure 2 b). Similarly, the minimum height of the fibers formed in 1-hexanol was ca. 60 nm (Figure 2 c, d). The fibers with a height of ca. 60 nm assembled to form bundles with width of ca. 200 nm (Figure 2 e), which hierarchically formed right-handed helical structures with a width of $\sim 1 \mu\text{m}$.

3.2 X-ray diffraction analysis of organogels. Next, using X-ray diffraction, we investigated the structure of the fibers in the gels (Figure S4). A characteristic peak ($d = 5.5 \text{ nm}$) was observed on the X-ray diagrams of all the gels; this peak was attributable to the long period. Two more peaks ($d = 2.8$ and 1.4 nm) were observed; these likely represented 1/2 and 1/3 reflection peaks of the long period. The diffraction patterns of all the fibers formed from 16AG suggested formation of lamellar structures with a long period of ca. 5.5 nm which corresponds to approximately twice the short axis of 16AG molecule; this result was similar to that for fibers formed from 16AG in paraffin.³³ Therefore, two 16AG molecules likely associate and form disk-like aggregates in alcohol solvents.³³

3.3 Measurement for sol-to-gel transition temperature of organogels. The kind of alcohol also affected the phase transition behavior of gels formed from 16AG. Using

variable-temperature transmission spectroscopy, we evaluated the Tgel of 16AG in alcohols (Table 1, Figure 3). The transmittances of the alcohol solutions containing 16AG decreased sharply in a narrow temperature range upon cooling, suggesting that sol-to-gel phase transition occurred highly cooperatively in all alcohols. However, the Tgel differed in each alcohol, for instance, it was 54°C in methanol, 55°C in ethanol, 47°C in 1-propanol, and 35°C in 1-decanol. Thus, the Tgel decreased gradually with an increase in the number of carbons. The plot of Tgel and E_T^N displayed linear correlation between empirical polarity parameter³⁵ $E_T^N = 0.654$ (ethanol) to $E_T^N = 0.525$ (1-decanol) as shown in Figure 3, inset.

Figures 1 - 3

3.4 Gelation behavior of 16AG in ethanol / 1-hexanol mixture solvents. The above findings show that the decrease in polarity resulted in a decrease in the pitch of the helical fibers and in Tgel. Next, we investigated the organogelation of 16AG in solvent mixtures containing ethanol ($E_T^N = 0.654$) and 1-hexanol ($E_T^N = 0.559$) at various volume ratios. Optical microscopy images showed that the pitch of the helical fibers depended on the ethanol : 1-hexanol ratio (Figure 4, Figure S1 k~o). The mean pitch values from 20 measurements were 3.1 μm (ethanol : 1-hexanol, 8 : 2), 2.6 μm (6 : 4), 2.3 μm (5 : 5), 1.4 μm (4 : 6), and 1.2 μm (2 : 8), i.e., the pitch decreased with the decreasing polarity of the solvent (Table 1, lower part, Figure S3 b). Using variable-temperature transmittance spectroscopy, we evaluated the Tgel of 16AG in ethanol : 1-hexanol mixtures (Figure 5). The Tgel decreased with decreasing solvent polarity; for example, it was 49°C at the 8 : 2 ratio and 40°C at the 2 : 8 ratio. Thus,

controlling solvent polarity enabled us to finely tune the helical pitch of the fibers and Tgel of supramolecular organogels formed from 16AG. Using variable-temperature circular dichroism (CD) spectroscopy, we further investigated the structural differences between fibers formed in ethanol and 1-hexanol. In tetrahydrofuran (good solvent for 16AG), a CD spectrum of 16 AG showed a negative band at $\lambda = 200$ nm (Figure S5), the absorption region of ester moiety.³⁶ A bisignate CD signal with a zero crossing at $\lambda = 200$ nm was observed in 1-hexanol at 40°C to 80°C (Figure 6 a). The intensity of the negative CD band at $\lambda = 220$ nm was increased gradually by cooling from 80°C to 50°C, and was decreased by subsequent cooling to 40°C (Figure 6 a inset). Although the solution of 16AG in 1-hexanol remained transparent and displayed no-changes in the transmittance spectrum during cooling from 80°C and 50°C (Figure 3), the exciton-coupled CD signal distinct from that in tetrahydrofuran strongly indicated that a helical pre-aggregate of 16AG was formed in the sol state.³⁷ A drastic change was observed in the shape of the CD signal after cooling to 35°C (below the Tgel): a positive CD band appeared with a maximum at $\lambda = 240$ nm and a broad shoulder (Figure 6 a and inset). In contrast, an organogel formed in ethanol showed neither such an intense CD signal nor changes upon cooling (Figure 6 b).

Figures 4 - 6

3.5 Proposed mechanism of the formation of supramolecular helical fibers. We propose a mechanism of the formation of supramolecular helical fibers in organogels formed from 16AG and alcohol solvents (Figure 7). First, 16AG molecules dissolved in alcohol solvent at a high temperature form pre-aggregates due to the solvophobic effect.

The decrease in T_{gel} with the decreasing polarity of the alcohol solvent used suggests that the pre-aggregates are more stable at lower solvent polarity. As the CD spectrum of 16AG in 1-hexanol shows (Figure 6 a), the pre-aggregates are CD-active even in the sol state, and their chirality is amplified with decreasing temperature. The helical molecular arrangement should be more advantageous in solvents with lower polarity because the palmitoyl chains that form the exterior of the aggregate more effectively prevent the access of solvent molecules to the polar ester and ether moieties of 16AG (Figure S6). The shape of the CD signal changed dramatically below the T_{gel} , suggesting a rapid formation of higher-order helical structures, as observed in atomic force microscopy images (Figure 2b). In contrast to 1-hexanol, in ethanol 16AG produced no intense CD signals, suggesting hierarchical formation of non-helical fibers from non-helical pre-aggregates. These results revealed that the chirality of the pre-aggregates formed in the sol state has a strong effect on the chirality of the higher-order structures such as non-helical tapes and helical fibers that constitute supramolecular organogels, and that the stability and chirality of the pre-aggregates vary with solvent polarity.

Figure 7

4 Conclusions

In conclusion, we demonstrated that palmitoylated 1,5-anhydro-D-glucitol (16AG) is able to gelatinize various primary alcohols and that the structure and phase transition temperature of the supramolecular fibrous gels formed from 16AG vary depending on the solvent used: helical fibers were formed in alcohols composed of three carbons or

more (1-propanol), and the helical pitch and phase transition temperature decreased gradually with increasing number of carbons in the alcohols (decreasing polarity). The helical pitch and transition temperature of the gels obtained in ethanol : 1-hexanol mixtures were tunable by changing the ratio of these solvents. Thus, we demonstrated that the morphology and phase transition temperature of supramolecular fibrous gels formed from 16AG are sensitive to the polarity of the alcohol solvent. The present study provides a strategy for precise tuning of morphology and physicochemical properties of organogels formed from low-molecular-weight gelators, and will contribute to the development for soft materials chemistry.

Acknowledgements

We thank Dr. H. Minamikawa of the National Institute of Advanced Industrial Science and Technology (AIST) for his help with the XRD measurements. R. I. is supported in part by a Grant-in-Aid for Scientific Research (19K05177) from the Japan Society for the Promotion of Science (JSPS). R. I. and S. K. are supported by Adaptable and Seamless Technology transfer Program through Target-driven R&D (A-STEP) from Japan Science and Technology Agency (JST).

Keywords: Fibers, Helical structures, Self-assembly, Solvent effects, Supramolecular chemistry

Conflict of interest

The authors declare no conflict of interest.

Electronic Supplementary Information

ESI is available.

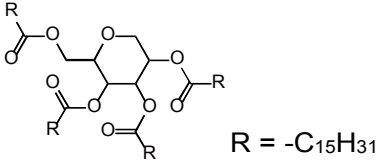
References

1. L. Zhang, T. Wang, Z. Shen and M. Liu, *Adv. Mater.*, 2016, **28**, 1044-1059.
2. E. Yashima, N. Ousaka, D. Taura, K. Shimomura, T. Ikai and K. Maeda, *Chem. Rev.*, 2016, **116**, 13752-13990.
3. M. A. Mateos-Timoneda, M. Crego-Calama and D. N. Reinhoudt, *Chem. Soc. Rev.*, 2004, **33**, 363-372.
4. M. Ikeda, *Bull. Chem. Soc. Jpn.*, 2013, **86**, 11-24.
5. Y. Dorca, E. E. Greciano, J. S. Valera, R. Gomez and L. Sanchez, *Chem. Eur. J.*, 2019, **25**, 5848-5864.
6. D. N. Nadimetla, M. Al Kobaisi, S. T. Bugde and S. V. Bhosale, *Chem Rec*, 2020, **20**, 793-819.
7. M. L. Mason, R. F. Lalisce, T. J. Finnegan, C. M. Hadad, D. A. Modarelli and J. R. Parquette, *Langmuir*, 2019, **35**, 12460-12468.
8. P. Y. Xing and Y. L. Zhao, *Acc. Chem. Res.*, 2018, **51**, 2324-2334.
9. G. F. Liu, X. Li, J. H. Sheng, P. Z. Li, W. K. Ong, S. Z. F. Phua, H. Agren, L. L. Zhu and Y. L. Zhao, *Acs Nano*, 2017, **11**, 11880-11889.
10. B. Adhikari, J. Nanda and A. Banerjee, *Soft Matter*, 2011, **7**, 8913-8922.
11. I. Danila, F. Riobe, F. Piron, J. Puigmarti-Luis, J. D. Wallis, M. Linares, H. Agren, D. Beljonne, D. B. Amabilino and N. Avarvari, *J. Am. Chem. Soc.*, 2011, **133**, 8344-8353.
12. F. Pop, C. Melan, I. Danila, M. Linares, D. Beljonne, D. B. Amabilino and N.

- Avarvari, *Chem. Eur. J.*, 2014, **20**, 17443-17453.
13. S. C. Karunakaran, B. J. Cafferty, A. Weigert-Munoz, G. B. Schuster and N. V. Hud, *Angew. Chem. Int. Ed.*, 2019, **58**, 1453-1457.
 14. G. Liu, J. Liu, C. Feng and Y. Zhao, *Chem Sci*, 2017, **8**, 1769-1775.
 15. S. J. George, R. de Bruijn, Z. Tomovic, B. Van Averbek, D. Beljonne, R. Lazzaroni, A. P. Schenning and E. W. Meijer, *J. Am. Chem. Soc.*, 2012, **134**, 17789-17796.
 16. S. Xue, P. Xing, J. Zhang, Y. Zeng and Y. Zhao, *Chemistry*, 2019, **25**, 7426-7437.
 17. P. Jonkheijm, P. van der Schoot, A. P. Schenning and E. W. Meijer, *Science*, 2006, **313**, 80-83.
 18. Y. Sun, C. He, K. Sun, Y. Li, H. Dong, Z. Wang and Z. Li, *Langmuir*, 2011, **27**, 11364-11371.
 19. P. Duan, Y. Li, L. Li, J. Deng and M. Liu, *J. Phys. Chem. B*, 2011, **115**, 3322-3329.
 20. J. Cui, J. Zheng, W. Qiao and X. Wan, *J. Colloid Interface Sci.*, 2008, **326**, 267-274.
 21. D. Mandal, S. Dinda, P. Choudhury and P. K. Das, *Langmuir*, 2016, **32**, 9780-9789.
 22. C. Liu, Q. Jin, K. Lv, L. Zhang and M. Liu, *Chem. Commun.*, 2014, **50**, 3702-3705.
 23. S. P. Goskulwad, M. Al Kobaisi, D. D. La, R. S. Bhosale, M. Ratanlal, S. V. Bhosale and S. V. Bhosale, *Chem. Asian J.*, 2018, **13**, 3947-3953.
 24. D. A. Shejul, S. M. Wagalgave, R. W. Jadhav, M. Al Kobaisi, D. D. La, L. A.

- Jones, R. S. Bhosale, S. V. Bhosale and S. V. Bhosale, *New J. Chem.*, 2020, **44**, 1615-1623.
25. Y. Hu, S. G. Xu, K. Miao, X. R. Miao and W. L. Deng, *PCCP*, 2018, **20**, 17367-17379.
26. Z. W. Zhang, S. Z. Zhang, J. J. Zhang, L. L. Zhu and D. H. Qu, *Tetrahedron*, 2017, **73**, 4891-4895.
27. M. A. Gillissen, M. M. Koenigs, J. J. Spiering, J. A. Vekemans, A. R. Palmans, I. K. Voets and E. W. Meijer, *J. Am. Chem. Soc.*, 2014, **136**, 336-343.
28. Y. Nagata, T. Nishikawa, M. Sugimoto, S. Sato, M. Sugiyama, L. Porcar, A. Martel, R. Inoue and N. Sato, *J. Am. Chem. Soc.*, 2018, **140**, 2722-2726.
29. V. V. Borovkov, G. A. Hembury and Y. Inoue, *Angew. Chem. Int. Ed.*, 2003, **42**, 5310-5314.
30. Q. Jin, L. Zhang and M. Liu, *Chem. Eur. J.*, 2013, **19**, 9234-9241.
31. Y. M. Zhang, S. Y. Li, M. F. Ma, M. M. Yang, Y. J. Wang, A. Y. Hao and P. Y. Xing, *New J. Chem.*, 2016, **40**, 5568-5576.
32. Y. Y. Mao, K. Y. Liu, L. Y. Meng, L. Chen, L. M. Chen and T. Yi, *Soft Matter*, 2014, **10**, 7615-7622.
33. T. Kajiki, S. Komba and R. Iwaura, *ChemPlusChem*, 2020, **85**, 701-710.
34. T. Kajiki and S. Komba, *J. Apply. Glycosci.*, 2019, **66**, 103-112.
35. C. Reichardt, *Chem. Rev.*, 1994, **94**, 2319-2358.
36. L. Dorfman, *Chem. Rev.*, 1953, **53**, 47-144.
37. N. Berova, K. Nakanishi and R. W. Woody, *Circular Dichroism: Principles and Applications 2nd Ed.*, Wiley-VCH, New York, 2000.

Table 1 Gelation properties and normalized empirical polarity parameter, E_T^N , of alcohol solvents.



$R = -C_{15}H_{31}$

Gelator 16AG				
Solvent	Appearance	Helical pitch (μm) ^c	Sol-to-gel transition temperature ($^{\circ}\text{C}$)	E_T^N
Methanol	Solid	– ^d	54	0.762
Ethanol	VOG ^a	– ^d	55	0.654
1-Propanol	OG ^b	3.3	47	0.617
1-Butanol	OG ^b	1.6	42	0.586
1-Pentanol	OG ^b	1.4	41	0.586
1-Hexanol	OG ^b	1.3	40	0.559
1-Heptanol	OG ^b	1.2	37	0.549
1-Octanol	OG ^b	1.1	36	0.537
1-Nonanol	OG ^b	1.0	35	0.528
1-Decanol	OG ^b	1.2	35	0.525

Ethanol : 1-hexanol				
(v/v)				
8 : 2	VOG ^a	3.1	49	–
6 : 4	OG ^b	2.6	47	–
5 : 5	OG ^b	2.3	43	–
4 : 6	OG ^b	1.4	42	–
2 : 8	OG ^b	1.2	40	–

^a Very opaque gel, ^b opaque gel, ^c mean values from 20 measurements on optical microscopy images, ^d most fibers showed non-helical morphology.

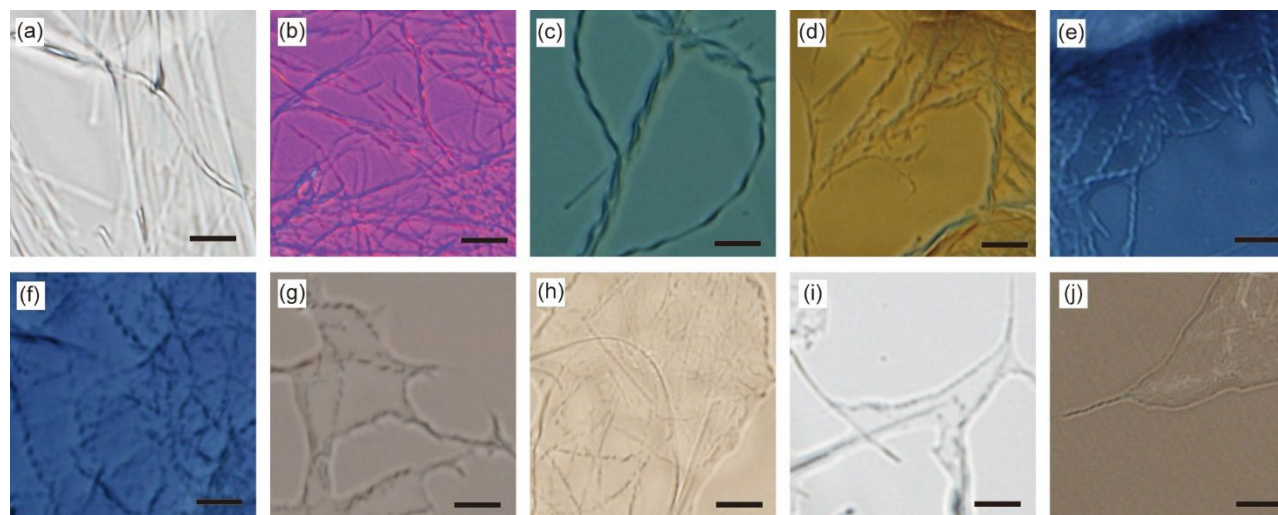


Figure 1 Optical microscopy images of organogels formed from 1,5-anhydro-2,3,4,6-tetra-*O*-palmitoyl-D-glucitol (16AG) in (a) methanol, (b) ethanol, (c) 1-propanol, (d) 1-butanol, (e) 1-pentanol, (f) 1-hexanol, (g) 1-heptanol, (h) 1-octanol, (i) 1-nonanol, and (j) 1-decanol. Scale bars = 5 μm .

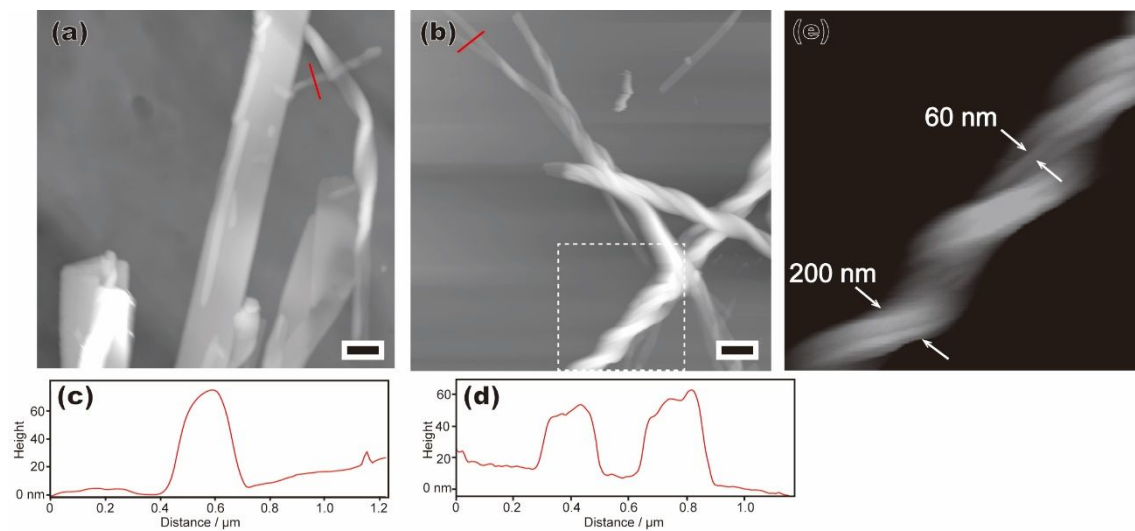


Figure 2 Atomic force microscopy images of fibers formed from 16AG in (a) methanol and (b) 1-hexanol; height profiles along the red lines in (a) and (b) are shown in (c) and (d), respectively. (e) A magnified image of the area within the dotted square in (b). Scale bars = 1 μm .

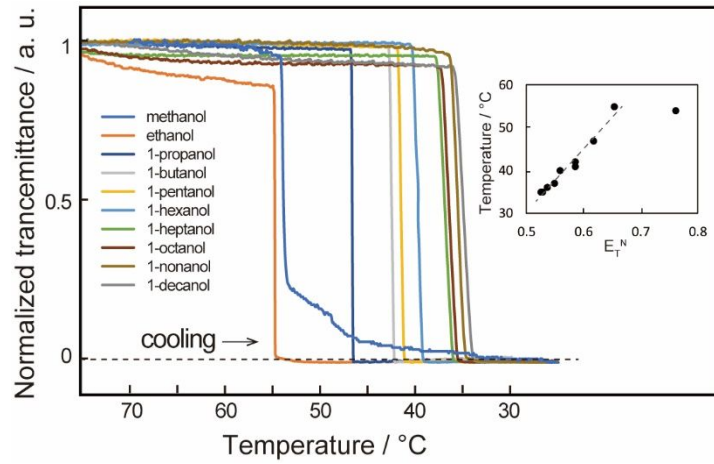


Figure 3 Temperature-dependent changes in transmittance of organogels formed from 16AG in the indicated alcohols. Transmittance was measured at $\lambda = 500$ nm and was normalized to the maximal transmittance of each sample. Inset shows a plot of sol-to-gel transition temperature of 16AG in each alcohol versus E_T^N parameter of the alcohol used.

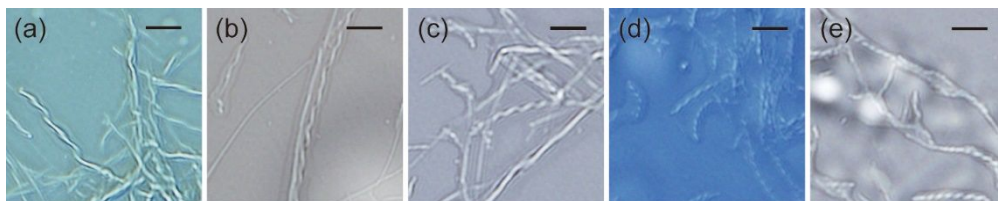


Figure 4 optical microscopy images of supramolecular fibers formed from 16AG in ethanol : 1-hexanol mixtures (v/v): (a) 8 : 2, (b) 6 : 4, (c) 5 : 5, (d) 4 : 6, and (e) 2 : 8. Scale bars = 5 μm .

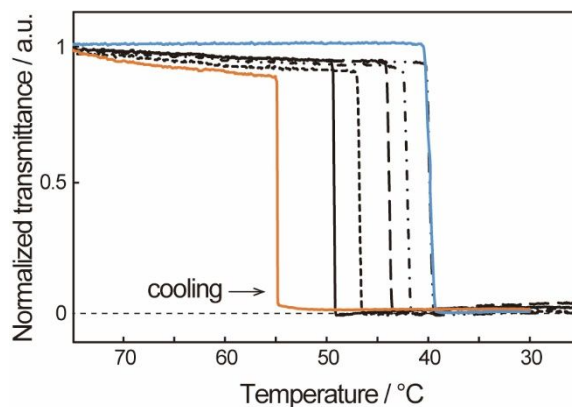


Figure 5 Temperature dependence of the transmittance of organogel formed upon cooling from 16AG in ethanol (orange line), ethanol : 1-hexanol mixtures (v/v) 8 : 2 (—), 6 : 4 (----), 5 : 5 (— — —), 4 : 6 (·—·—·), 2 : 8 (·—·—·—·), and 1-hexanol (blue line). Transmittance was measured at 500 nm and was normalized to the maximal transmittance of each sample.

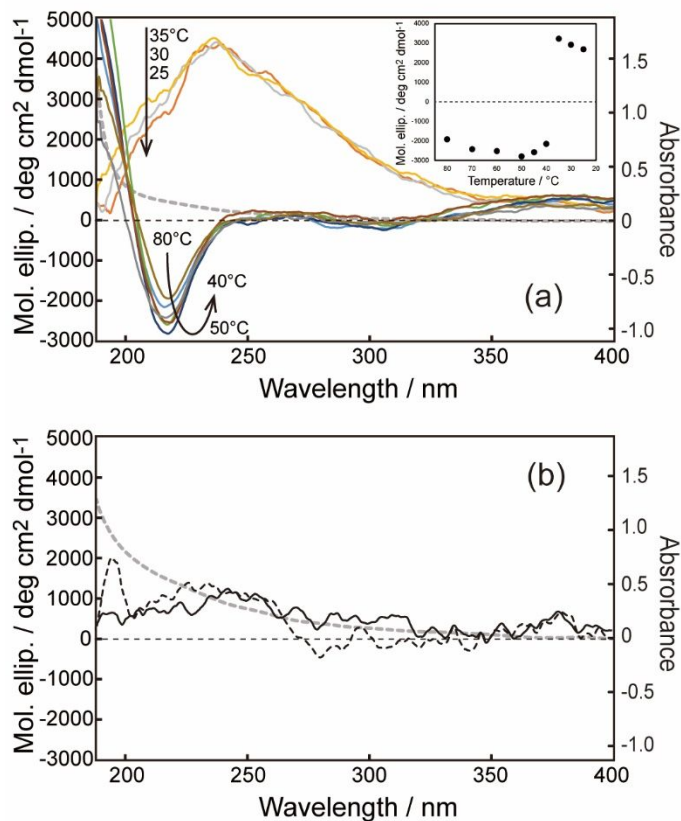


Figure 6 (a) Temperature dependence of circular dichroism spectra of organogel formed from 16AG in 1-hexanol. Inset shows a plot of molecular ellipticity at $\lambda = 220$ nm versus temperature, and (b) circular dichroism spectra of organogel formed in ethanol at 25 (black dotted line) and 68°C (black line). For reference, an absorption spectrum measured in each solvent is indicated as dotted gray line.

Table of Contents Entry

The pitch of supramolecular helical fibers formed from palmitoylated 1,5-anhydro-D-glucitol was able to be tuned by controlling the polarity of alcohol solvent.

